

## Article

# Single Pulse Studies of PSR B0950+08 with FAST

Heng Yang <sup>1,2</sup>, Shijun Dang <sup>1,2,\*</sup>, Qijun Zhi <sup>1,2,\*</sup>, Lunhua Shang <sup>1,2</sup>, Xin Xu <sup>1,2</sup>, Dandan Zhang <sup>1,2</sup>, Shuo Xiao <sup>1,2</sup>, Rushuang Zhao <sup>1,2</sup>, Aijun Dong <sup>1,2</sup> , Hui Liu <sup>1,2</sup>, Ziyi You <sup>1,2</sup> , Qingying Li <sup>1,2</sup>, Yuanyi Qin <sup>1,2</sup>, Yanqing Cai <sup>1,2</sup> and Wei Li <sup>1,2</sup>

<sup>1</sup> School of Physics and Electronic Science, Guizhou Normal University, Guiyang 550025, China

<sup>2</sup> Guizhou Provincial Key Laboratory of Radio Astronomy and Data Processing, Guizhou Normal University, Guiyang 550025, China

\* Correspondence: dangsj@gznu.edu.cn (S.D.); qjzhi@gznu.edu.cn (Q.Z.)

**Abstract:** We report detailed polarization and single-pulse studies of PSR B0950+08 with the Five-hundred-meter Aperture Spherical Radio Telescope (FAST) at 1250 MHz. Significant bridge emission was observed between the inter-pulse and the main pulse and the height of the bridge decreased with increase in frequency. Our results support the interpretation that both the inter-pulse and the main pulse of this pulsar are from the same magnetic pole. From the relative peak flux density and the relative energy distribution, we conclude that no giant pulse was detected in PSR B0950+08. Our results provide opportunities to study the origin of the emission from PSR B0950+08 and offer new insights into the origins of pulsar emission and bridge emission.

**Keywords:** star; neutron pulsar; radio pulsar; PSR B0950+08 (J0953+0755)

## 1. Introduction

PSR B0950+08 (J0953+0755) is a bright pulsar with a pulse period of 253 ms. This pulsar is famous for its bridge emission between the main pulse (MP) and inter-pulse (IP) and its giant pulse (GP) emission. Using the Arecibo telescope, Hankins & Cordes [1] carried out a detailed study of the bridge emission between the MP and the IP of PSR B0950+08 for the first time. They found that the IP of this pulsar was correlated with the MP and that the inter-pulse–main-pulse separation was frequency-independent between 100 and 5000 MHz. Bilous et al. [2] found that the bridge emission was more obvious at low frequencies. These unique physical phenomena of PSR B0950+08 have stimulated research on whether the IP of pulsars comes from a single magnetic pole or opposite magnetic poles. The physical connection between the bridge emission and the MP and IP remains a mystery and the origin of the bridge emission is still unknown.

It is generally believed that the radio emission of pulsars originates from the polar cap region of the neutron star. The study of single pulses can help us to understand the unique physical phenomena in the emission region of pulsars, such as pulse mode change, nulling, sub-pulse drifting, and giant pulses. The pulse mode change is the average profile of pulsars when changed between two or more stable profile shapes [3]. Nulling is a phenomenon in which the pulse disappears in a period of time (usually several thousands of pulse cycles) and can then be detected by the telescope [4]. Sub-pulse drifting occurs where a sub-pulse changes regularly and moves forward or backward at a specific rate in the pulse window [5]. The GP is a short duration, very bright, pulse emission from a pulsar [6–10]. A GP often occurs in narrow phase windows, the energy exceeding the average pulse energy by 10 times or even much more. To date, only 16 pulsars have been detected exhibiting the remarkable GP phenomenon [11–17]. Generally, the energy distribution of normal pulses follows a normal or log-normal distribution. However, the energy distribution of the GP is different from that of a normal pulse and follows a power-law distribution [18,19]. The difference in pulse energy distribution means that normal pulses and a GP have different emission



**Citation:** Yang, H.; Dang, S.; Zhi, Q.; Shang, L.; Xu, X.; Zhang, D.; Xiao, S.; Zhao, R.; Dong, A.; Liu, H.; et al. Single Pulse Studies of PSR B0950+08 with FAST. *Universe* **2023**, *9*, 50. <https://doi.org/10.3390/universe9010050>

Academic Editor: Liyun Zhang

Received: 15 December 2022

Revised: 10 January 2023

Accepted: 10 January 2023

Published: 12 January 2023



**Copyright:** © 2023 by the authors. Licensee MDPI, Basel, Switzerland. This article is an open access article distributed under the terms and conditions of the Creative Commons Attribution (CC BY) license (<https://creativecommons.org/licenses/by/4.0/>).

mechanisms [20–22]. The GP of PSR B0950+08 has been reported in a number of papers (e.g., [23–25]), with a criterion of 30 times the peak flux density of an average pulse (AP) usually selected as the threshold to judge whether the single pulse is a GP.

Using the Rajkot radio telescope, Singal et al. observed PSR B0950+08 at 103 MHz and detected one million pulses [19]. They found that there was high energy variability at low frequency (which is usually considered as a GP) and that single pulses with energy 100 times greater than the average pulse energy accounted for about 1% of the received single pulses. Subsequently, Cairns et al. [26] reported that the single pulse emission of PSR B0950+08 exhibited several components, such as GP emission, giant micro-pulse emission, and other components. The energy of these emission components follows the power-law distribution, with the power-law index differing between them. It is difficult to clearly distinguish GP and giant micro-pulses based on observations of PSR B0950+08 at low frequency with insufficient observation time; observations at high frequencies are very important to enable such conclusions to be drawn. Smirnova [27] analyzed single pulses of PSR B0950+08 at 112 MHz and found that the maximum peak flux density of a single pulse reached 15,240 Jy and that the energy of this single pulse exceeded the average pulse energy by a factor of 153. Singal and Vats [28] observed PSR B0950+08 continuously for about 10 months at 103 MHz and found that the frequency of incidence of GPs of this pulsar was the highest among known pulsars. The flux density level of the continuous GP fluctuated rapidly and the frequency of the incidence rate of these GPs for observations for consecutive days underwent a large change. Tsai et al. [25] reported the detection of GP emission of PSR B0950+08 simultaneously at 42 and 74 MHz in 12 h of observations using the first station of the Long Wavelength Array, LWA1. They detected 275 and 465 GPs at 42 and 74 MHz, respectively; the flux density of the GP was considered to be more than 10 times that of the average pulse (AP). The cumulative distribution of the pulse intensity of GPs followed the power law. The Amsterdam-ASTRON Radio Transient Facility and Analysis Centre (AARTFAAC) was used by Kuiack et al. [23] to observe PSR B0950+08 with variable height and detected extreme GPs at 58.3 and 61.8 MHz. These authors obtained some samples of 275 pulses, of which the brightest pulses were one order of magnitude brighter than the pulse reported by Tsai et al. [25] at 42 and 72 MHz, consistent with the results obtained from the previous long-term observation at 103 MHz. In previous studies on GPs, it was found that their rate and fluence distribution were different. The GP rate was found to be highly variable, from 0 to 30 per hour; only two three-hour observations accounted for approximately half of the pulses detected in the 96 h of observation. Recently, based on observations at 55 MHz (NenuFAR) and 1.4 GHz (Westerbork Synthesis Radio Telescope), Bilous et al. [2] concluded that PSR B0950+08 did not emit GPs and pointed out that the previously reported GP emission in PSR B0950+08 may have been caused by using the non-contemporary average flux density to normalize the GP energy [2]. The issue of whether PSR B0950+08 has GP emissions or not mainly reflects the fact that the previous observation sensitivity was too low to precisely determine its average profile component. Hence, it is necessary to carry out a high-sensitivity polarization observation on PSR B0950+08 to provide better observational evidence to determine its emission mechanism.

In this study, we used the unique advantages of the FAST telescope to carry out a detailed single-pulse polarization analysis on PSR B0950+08. The observations and data processing undertaken are shown in Section 2. In Section 3, we present the observation results, mainly including the average polarization profile and single-pulse characteristics, which are discussed in Section 4 and summarized in Section 5.

## 2. Observations and Data Processing

We observed PSR B0950+08 with the Five-hundred-meter Aperture Spherical Radio Telescope (FAST) in Guizhou Province, China, on 26 November 2019 (corresponding to MJD 58812). The data were collected by the central beam of a 19-beam receiver with a central frequency of 1250 MHz and recorded by a digital backend based on the Reconfigurable Open-architecture Computing Hardware-version2 (ROACH2) [29] with four polarizations. The corresponding bandwidth was 400 MHz, the frequency channel was 4096, and the sample interval was 49.152- $\mu$ s. A total of 14,232 single pulses were obtained during 1 h of observation. A stable noise signal with a period of 0.201326592 s was injected by a single diode to calibrate the data.

For the offline data process, the detailed processing steps were as follows: Firstly, based on the timing ephemeris provided by PSRCAT-V1.57 [30], we folded the data using the DSPSR [31] to obtain single-pulse profiles with 1024 phase bins for each pulse. Secondly, we automatically removed the radio-frequency interference (RFI) in the frequency domain and removed 5 % of the band-edges using the median smoothed difference algorithm of the PAZ plugin of the PSRCHIVE software package [31]. Thirdly, the polarization was calibrated using the PAC plugin of the PSRCHIVE software package. Finally, to investigate the frequency dependence of the pulse profile, we split the profiles into three unequal sub-bands using the PAZ plugin.

## 3. Results

### 3.1. Average Profile

A large number of observations previously undertaken have indicated that the average radio pulse profile of PSR B0950+08 is composed of IP and MP components [1,2]. Hankins and Cordes [1] found, using the Arecibo telescope, that the average pulse profile of PSR B0950+08 involved obvious bridge emissions between the IP and the MP at 400 MHz. Cairns et al. [26], using the Parkes telescope, found the precursor component before MP was 400–1400 MHz. Recently, Bilous et al. [2] carried out multi-band observations of the pulsar using the NenuFAR and Westerbork Synthesis radio telescopes and found that there was a certain frequency dependence on the separation of the precursor from the MP and that the separation at low frequencies was larger than at high frequencies. In addition, the bridge emissions between the IP and MP varied with frequency and the intensity of emissions at lower frequencies was stronger than at high frequencies.

In this study, we carried out radio observations of PSR B0950+08 at 1250 MHz. Figure 1 shows the average polarized pulse profile of PSR B0950+08. Panel (a) shows the position angles of the linear polarization (PPA), panel (b) shows the average pulse profile, while panels (c) and (d) indicate  $\times 100$  and  $\times 1000$  times the extent for panel (b), respectively, where the pulse profile has been normalized. The average profile of the pulsar is mainly composed of IP and MP components (for ease of comparison with previous work, we continue to use this name in the following discussion). We also detected a significant bridge emission component between the MP and IP (see panels (c) and (d) of Figure 1) at 1250 MHz. Furthermore, from the pulsar longitude  $50^\circ$ – $360^\circ$ , we detected an obvious PPA swing, while components other than the PAA swing were not detected (this area corresponds to the off-pulse window and is represented by a gray region). The shape of the PPA swing was similar to that reported in [32] (see Figure 1 in [32]).

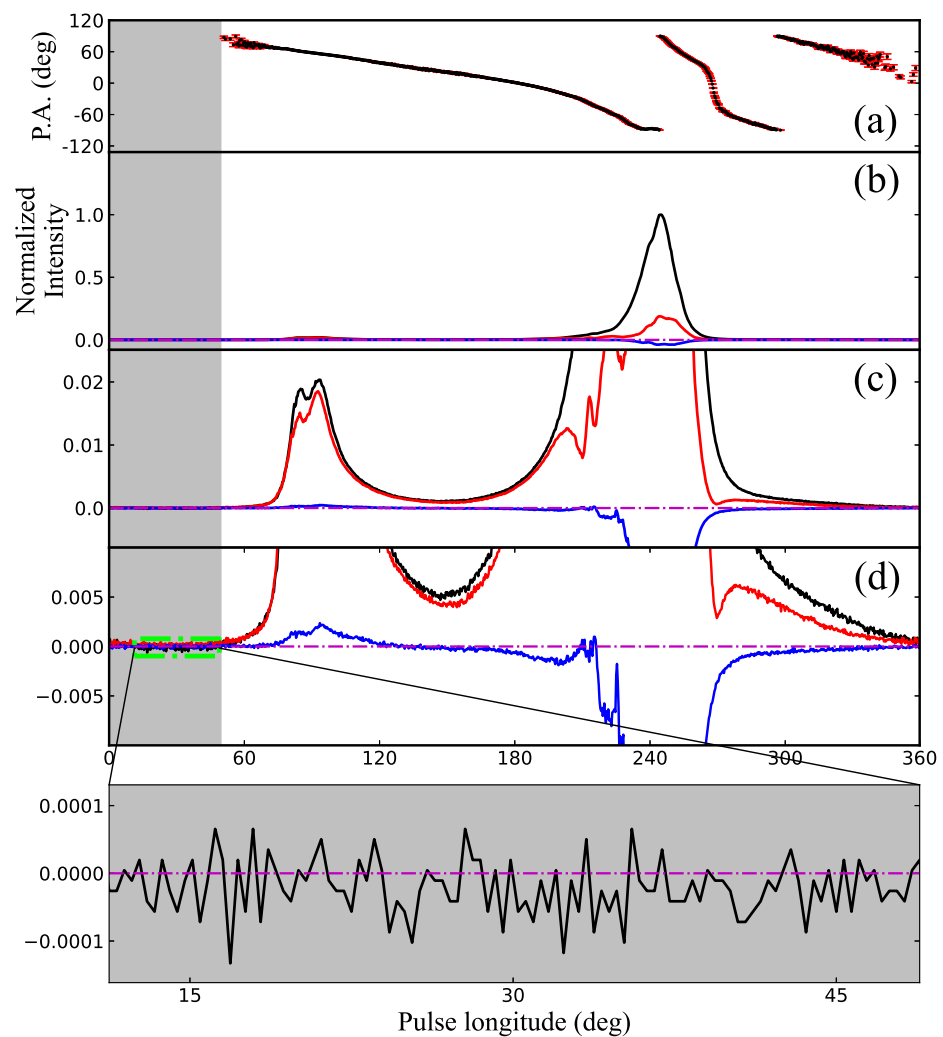


**Figure 1.** The polarized profile of PSR B0950+08. Panel (a) is the linear polarization position angle. Panel (b) is the polarized profile (the black, red and blue solid lines represent the total intensity, the linearly polarized intensity and the circularly polarized intensity, respectively). Panel (c) indicate  $\times 100$  times the extent for panel (b). The bottom panel shows the extent of the off-pulse window of the average pulse profile (the green square region of panel (d)).

The linear polarization intensity of PSR B0950+08 varies greatly in the pulse longitude of IP and MP. The leading component of IP has a low linear polarization intensity, while the tail component in IP has a strong linear polarization intensity. Similarly, the linear polarization of the leading component of MP is weaker than its trailing component. The circular polarization also varies significantly; its sign is negative in the MP and positive in the IP and the conversion of the sign occurs at the lowest point of the bridge emission. The insert in panel (d) shows the extent of the off-pulse window of the average pulse profile (the green square region). Obviously, the off-pulse window is dominated by noise. The horizontal magenta dotted line in the insert of panel (d) indicates that the pulse intensity is zero. The off-pulse window exhibits noise-like fluctuations. This indicates that there is an off-pulse window in PSR B0950+08, rather than emission in the entire pulse longitude. Our results support the interpretation that the pulse emission of PSR B0950+08 comes from the same magnetic pole (e.g., [1]).

### 3.2. The Frequency Dependence of Bridge Emission

It is very important to study the properties of bridge emission for investigate its emission geometry for pulsars with MP and IP (for example, whether the MP and IP

emissions come from a single magnetic pole or double magnetic poles). PSR B0950+08 is known for its bridge emission. However, limited by the sensitivity of the telescope used, previous observations only detected weak bridge emission between the MP and the IP [1]. Recently, Bilous et al. [2] found that the bridge emission of PSR B0950+08 is evolving with the observation frequency and becomes more significant at low frequencies (20–80 MHz). The high sensitivity of FAST provides a unique opportunity to study the characteristics of the bridge emission.

To study the frequency dependence of the bridge emission, we divided the bandwidth into three narrow-band frequencies, with corresponding center frequencies of 1105, 1225, and 1370 MHz. The bandwidths corresponding to these three frequencies were 110, 130, and 160 MHz, respectively. Here, the different bandwidths of the three frequencies were due to the elimination of the narrow-band RFI. Figure 2 shows the evolution of the bridge emission as a function of the three center frequencies. Panel (a) shows the average pulse profile at the three center frequencies. Panel (b) is  $\times 100$  times panel (a). The insert of panel (b) shows the extent of bridge emission. It is clear that the intensity of the bridge emission decreases when the frequency increases. This is consistent with the result of [2], i.e., that the bridge emission of PSR B0950+08 is more pronounced at low frequency. In addition, the intensity of the IP is also frequency-dependent, since it decreased with increase in frequency.

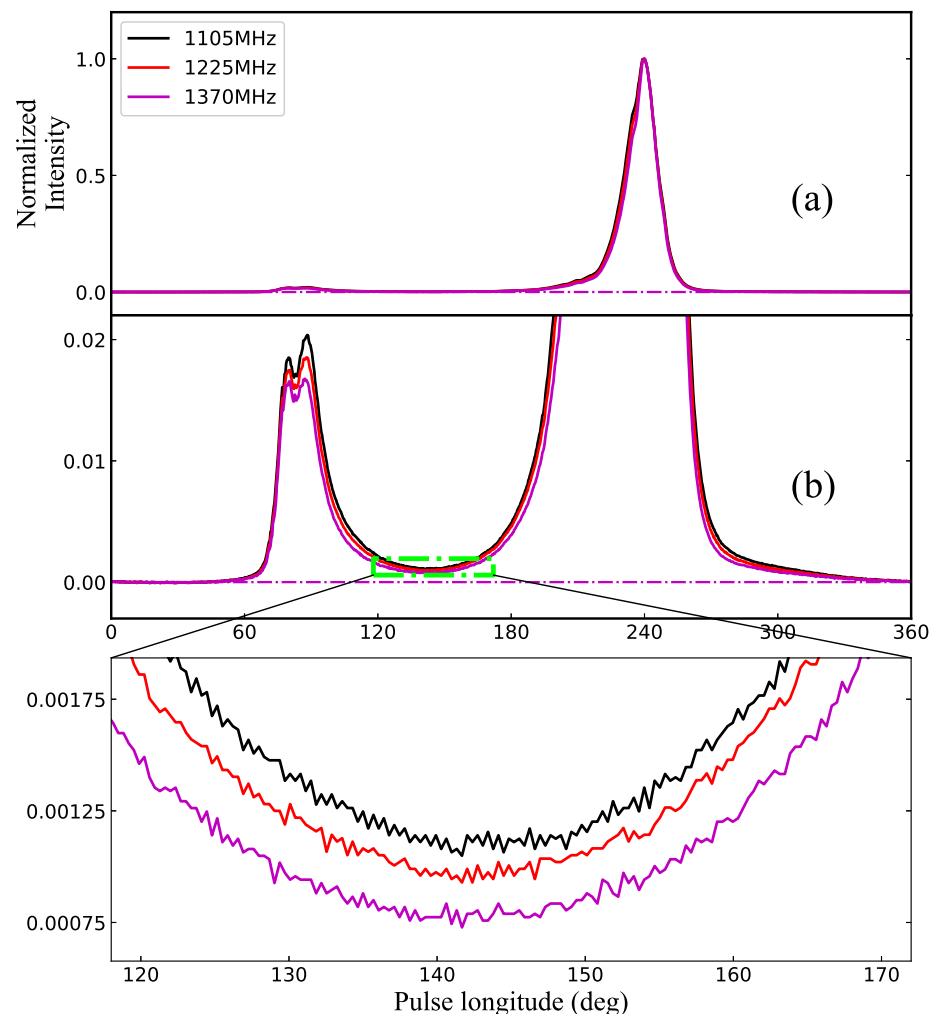


**Figure 2.** The frequency dependence of the average pulse profile. The average pulse profiles at 1105, 1225, and 1370 MHz are shown in the (a) panel with the black, red and magenta lines, respectively. The bottom panel is the extended green square region of panel (b).

### 3.3. The Single Pulse

In low-frequency observations, the high variability of the single pulse flux density and the energy of PSR B0950+08 is generally considered to result from GP or giant micro-pulses (e.g., [13,19,26,28,33]). However, based on observations at two widely separate frequencies, 55 MHz and 1.4 GHz, Bilous et al. [2] concluded that the single pulse of PSR B0950+08 was more similar to a normal pulse than the GP. The GP are usually defined as single pulses whose energy exceeds 10 times the average pulse energy or whose peak flux density exceeds 30 times the average pulse profile peak flux density [2,34]. The pulse energy for the GP usually follows a power-law distribution, while the pulse energy of normal pulses follow a normal or log-normal distribution [20]. A similar phenomenon occurs for the giant micropulses, in which the flux density is obviously greater than the typical value at unique pulse phases, but the overall integrated flux density of the profile is roughly the same [35]. This phenomenon has been detected in several young pulsars, such as the Vela pulsar and PSR J0901-4624 [21]. The energy density of the giant micro-pulses also follows a power-law distribution. Therefore, to verify whether PSR B0950+08 has a GP, we obtained the distribution of the relative peak flux density and the relative energy of the single pulse, respectively.

Figure 3 is the distribution of the relative peak flux density, and  $I_{Single}/I_{<AP>}$ , where  $I_{Single}$  is the peak flux density of each single pulse and  $I_{<AP>}$  is the peak flux density of the average pulse profile. It is obvious that the single pulse peak flux density of PSR B0950+08 is less than 20 times the average flux density across the entire on-pulse window. This is less than the peak flux intensity required to define a GP. Figure 4 is the distribution of the relative energy,  $E/<E>$ , of 14,232 single pulses. Here,  $E$  is the energy of each single pulse and  $<E>$  is the average energy of the whole on-pulse window. Obviously,  $E$  is less than six times  $<E>$ , which does not meet the criteria for a GP. Moreover, the off-pulse region (solid black line) follows the expected normal distribution and the on-pulse region follows a log-normal distribution, with the magenta dashed line being the best-fitting curve. This indicates that the energy distribution is consistent with the normal pulse. Therefore, our observation did not detect a GP at PSR B0950+08.

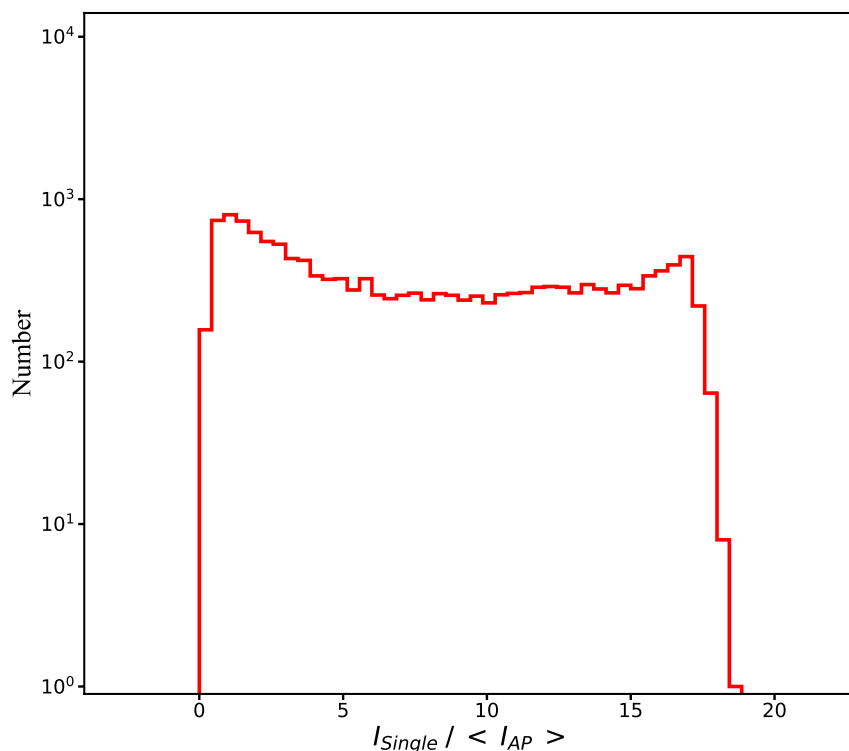


**Figure 3.** The distribution histogram of the pulse peak flux density. The peak flux density of each single-pulse ( $I_{Single}$ ) was normalized by the peak flux density of the average pulse profile ( $I_{AP}$ ).

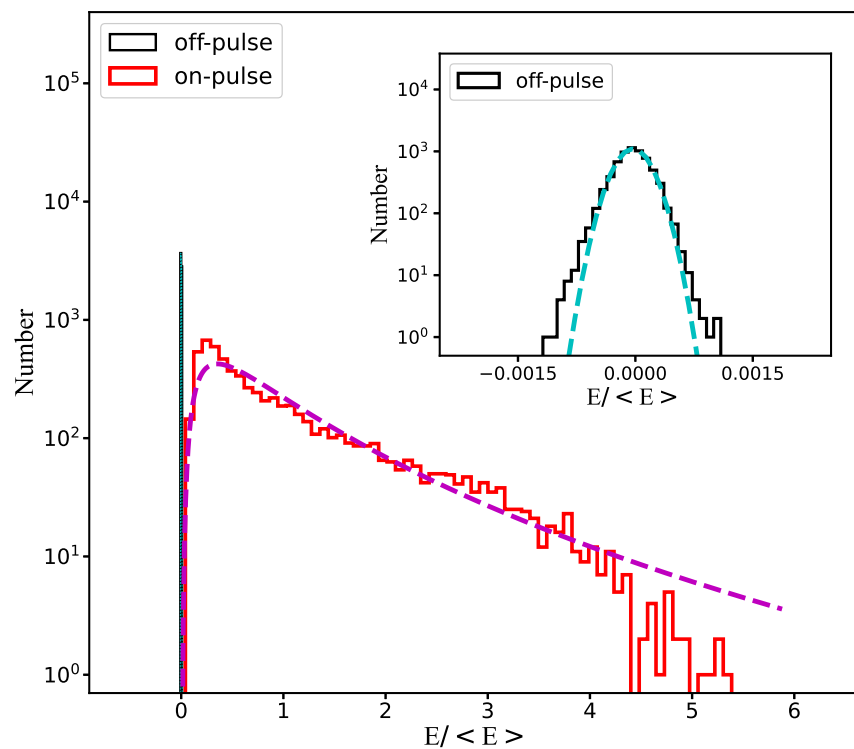


**Figure 4.** The relative energy distribution histogram of PSR B0950+08. The solid red and black lines represent the on-pulse and off-pulse regions, respectively. The energy of each single pulse was normalized by the average pulse energy. The magenta dashed line is a log-normal distribution fitted to the relative energy of all the pulses. The cyan dotted line in the insert panel is the off-pulse distribution.

#### 4. Discussion

As one of the earliest discovered bright pulsars with IP, PSR B0950+08 has been extensively studied for its average profile and single pulse features [35]. Previous research showed that the PPA of PSR B0950+08 varied from IP to MP. The PPA rotates continuously from IP to MP via bridge emission for a total rotation of nearly  $180^\circ$  (e.g., [1]). The initial interpretation of the  $180^\circ$  separation between IP and MP was that the pulsar may have an orthogonal geometric structure. The MP is generated in one polar cap and the IP in the other [36]. In addition, the IP can also be explained by a single magnetic pole model, where the IP and MP can occur in two possible scenarios [37–39]. In the first scenario, the emission in phase accounts for a large portion of the period; the IP and MP are from the two edges of the very wide emission beam. In the second scenario, the pulsar emits in a narrow emission beam, with the magnetic axis of the pulsar close to the rotation axis and the line of sight near the rotation axis. In the framework of orthogonal geometry, there is no bridge emission between IP and MP. However, our observations showed that there was an obvious bridge emission between the IP and the MP of PSR B0950+08 [1,2]. This conflicts with an orthogonal geometry interpretation and supports the single-pole model.

To date, it has been difficult to determine the origin of bridge pulses and whether they represent different pulse populations. Cairns, Iver H. [26] speculated that the bridge emission might be related to the giant micro-pulse of the pulsar, which was confirmed for the Vela pulsar [40]. Although bridge pulses can easily exceed the average emission in their respective phases, they are much weaker than MP or IP single pulses. In addition, they are easily overlooked using the standard practice of only investigating individual pulses in the pulse window. We expect more sensitive observation to provide further information on bridge pulses.

The intensity of a GP is powerful. The early study of the Crab pulsar found that some single pulses exhibit strong fluctuations in intensity and that the pulse intensity distributions exhibit a bimodal distribution (following a log-normal distribution for very weak single pulse intensities and a power-law distribution for strong single-pulse intensities) [22,41]. The Crab pulsar is prone to generate GPs; the initial statistical criterion for finding a GP is whether the pulse intensity distribution follows a power-law distribution. Similar phenomena have also been observed in other pulsars (e.g., [11,14–16,19]). Kazantsev et al. [42] reported that the generation of GPs from the Crab pulsar may be caused by the coherent instability of the plasma near the magnetic equator of the light cylinder (LC). Due to cyclotron instability, the radiative waves are amplified at frequencies close to the electron cyclotron harmonics. Although the emission region of the GP origin is still unknown, the pulse phase window seems to be associated with the components of the average profile, which is thought to be comprised of caustic radio waves emitted close to the LC. The high magnetic field strengths on the LC for the GP pulsars may be important for their emission mechanism (e.g., [43]). Depending on the magnetic field  $B_{lc}$  in the beam, GPs are usually generated from the strong magnetic field in the light beam, which occurs in some young pulsars and millisecond pulsars [13]. The magnetic field for PSR B0950+08 on the LC was calculated by Bilous et al., using the standard dipole magnetic field model, who found that the magnetic field on the LC of this pulsar was several orders of magnitude smaller than for other GP pulsars [2].

A large number of observations have indicated that PSR B0950+08 emits GPs at low frequencies (e.g., [19,26,27,34]). Recently, Bilous et al. [2] observed PSR B0950+08 at 55 MHz and 1.4 GHz and detected significant bridge emission, but no GP was detected. This can be attributed to the fact that only the energy of a part of the integrated pulse profile was selected to normalize the single pulse energy in previous GP studies. However, the existence of the bridge emission component makes it necessary to treat the main pulse, the inter-pulse, and the bridge component, as a whole. This will cause the value of the relative energy to be smaller than in previous reports. Using a similar method as Bilous et al. [2], we did not find any single-pulse whose peak flux density exceed 30 times the average pulse profile, or the relative energy of single-pulses that exceeded 10 times the average energy. Therefore, the intensity of the relative peak flux density and the energy of this pulsar did not meet the standard of GP. Our results also indicate that the energy distribution of PSR B0950+08 follows a log-normal distribution. This is similar to the energy distribution of normal pulses. Our results confirm that PSR B0950+08 may not have emitted GP. However, we cannot rule out that PSR B0950+08 does not emit GP (e.g., [28]) during this period. We expect to obtain more FAST observation time in the future to assess further whether this pulsar emits GP.

## 5. Summary

In this paper, we presented polarization observations of PSR B0950+08 with FAST at 1250 MHz. Our main findings were:

- (1) A significant bridge emission between the inter-pulse and the main pulse was detected.
- (2) The intensity of the bridge emission decreased with increase in frequency.
- (3) The interpretation that both MP and IP emissions of B0950+08 are from the same magnetic pole was supported.
- (4) There were no giant pulses detected in our observations.

Our results provide opportunities to investigate the origin of the emission from PSR B0950+08, as well as offering new insights into the origin of pulsar emission and bridge emission. However, much work remains to be undertaken to enable us to fully understand the emission mechanism and the structure of the magnetosphere of radio pulsars.

**Author Contributions:** Methodology, H.Y. and S.D.; data curation, H.Y., S.D. and X.X.; formal analysis, H.Y., S.D., L.S. and Q.Z.; software, H.Y., X.X., D.Z., S.X., H.L., Z.Y., Q.L., Y.Q., Y.C. and W.L.; validation, L.S., R.Z. and A.D.; writing—original draft, H.Y.; writing—review and editing, S.D.; funding acquisition, Q.Z. All authors have read and agreed to the published version of the manuscript.

**Funding:** This work was supported by the Guizhou Province Science and Technology Foundation (No. ZK[2022]304), the Scientific Research Project of the Guizhou Provincial Education (Nos. KY[2022]132, KY[2022]137), the National Natural Science Foundation (Grant Nos.: 12273008, U1731238, U1831120, U1838106, 61875087, 61803373, 11303069, 11373011, 11873080), the Foundation of Guizhou Provincial Education Department (No. KY (2020)003), the National Key R&D Program of China (No. 2017 YFB 0503300), the Foundation of Science and Technology of Guizhou Province (No. [2016]4008, [2017]5726-37, [2018]5769-02), and the Foundation of Guizhou Provincial Education Department (No. KY(2020)003).

**Data Availability Statement:** The data underlying this work are available in the FAST project 3044, and can be shared on request to the FAST Data Center. Follow this link (<https://fast.bao.ac.cn/cms/article/73/>) to find the source of the data.

**Acknowledgments:** We want to take this opportunity to thank the research advisors and reviewers for their comments. These comments were of great help in improving the paper. We have great expectations for future research. Our research work uses data from Five-hundred-meter Aperture Spherical radio Telescope. FAST is a Chinese national mega-science facility built and operated by the National Astronomical Observatories, the Chinese Academy of Sciences.

**Conflicts of Interest:** The authors declare no conflict of interest.

## References

1. Hankins, T.H.; Cordes, J.M. Interpulse emission from pulsar 0950+08: How many poles? *Astrophys. J.* **1981**, *249*, 241–253. [[CrossRef](#)]
2. Bilous, A.V.; Griefmeier, J.M.; Pennucci, T.; Wu, Z.; Bondonneau, L.; Kondratiev, V.; van Leeuwen, J.; Maan, Y.; Connor, L.; Oostrum, L.C.; et al. Dual-frequency single-pulse study of PSR B0950+08. *Astron. Astrophys.* **2022**, *658*, A143. [[CrossRef](#)]
3. Bartel, N.; Morris, D.; Sieber, W.; Hankins, T.H. The mode-switching phenomenon in pulsars. *Astrophys. J.* **1982**, *258*, 776–789. [[CrossRef](#)]
4. Wang, N.; Manchester, R.N.; Johnston, S. Pulsar nulling and mode changing. *Mon. Not. R. Astron. Soc.* **2007**, *377*, 1383–1392. [[CrossRef](#)]
5. Weltevrede, P.; Edwards, R.T.; Stappers, B.W. The subpulse modulation properties of pulsars at 21 cm. *Astron. Astrophys.* **2006**, *445*, 243–272. [[CrossRef](#)]
6. Bilous, A.V.; Pennucci, T.T.; Demorest, P.; Ransom, S.M. A Broadband Radio Study of the Average Profile and Giant Pulses from PSR B1821-24A. *Astrophys. J.* **2015**, *803*, 83. [[CrossRef](#)]
7. Knight, H.S.; Bailes, M.; Manchester, R.N.; Ord, S.M. A Study of Giant Pulses from PSR J1824-2452A. *Astrophys. J.* **2006**, *653*, 580–586. [[CrossRef](#)]
8. Lyutikov, M. On generation of Crab giant pulses. *Mon. Not. R. Astron. Soc.* **2007**, *381*, 1190–1196. [[CrossRef](#)]
9. McKee, J.W.; Stappers, B.W.; Bassa, C.G.; Chen, S.; Cognard, I.; Gaikwad, M.; Janssen, G.H.; Karuppusamy, R.; Kramer, M.; Lee, K.J.; et al. A detailed study of giant pulses from PSR B1937+21 using the Large European Array for Pulsars. *Mon. Not. R. Astron. Soc.* **2019**, *483*, 4784–4802. [[CrossRef](#)]
10. Sun, S.N.; Yan, W.M.; Wang, N. Detection of giant pulses in PSR J1047-6709. *Mon. Not. R. Astron. Soc.* **2021**, *501*, 3900–3904. [[CrossRef](#)]
11. Ershov, A.A.; Kuzmin, A.D. Detection of Giant Pulses from the Pulsar PSR B1112+50. *Astron. Lett.* **2003**, *29*, 91–95. [[CrossRef](#)]
12. Ershov, A.A.; Kuzmin, A.D. Detection of Giant Pulses in Pulsar PSR J1752+2359. *Chin. J. Astron. Astrophys.* **2006**, *6*, 30–33. [[CrossRef](#)]
13. Johnston, S.; Romani, R.W. Giant Pulses from PSR B0540-69 in the Large Magellanic Cloud. *Astrophys. J.* **2003**, *590*, L95–L98. [[CrossRef](#)]
14. Knight, H.S.; Bailes, M.; Manchester, R.N.; Ord, S.M. A Search for Giant Pulses from Millisecond Pulsars. *Astrophys. J.* **2005**, *625*, 951–956. [[CrossRef](#)]
15. Kuzmin, A.D.; Ershov, A.A. Giant pulses in pulsar PSR B0031-07. *Astron. Astrophys.* **2004**, *427*, 575–579. [[CrossRef](#)]
16. Kuzmin, A.D.; Ershov, A.A. Detection of giant radio pulses from the pulsar PSR B0656+14. *Astron. Lett.* **2006**, *32*, 583–587. [[CrossRef](#)]
17. Romani, R.W.; Johnston, S. Giant Pulses from the Millisecond Pulsar B1821-24. *Astrophys. J.* **2001**, *557*, L93–L96. [[CrossRef](#)]
18. Kuzmin, A.D. Giant pulses of pulsar radio emission. *Astrophys. Space Sci.* **2007**, *308*, 563–567. [[CrossRef](#)]
19. Singal, A.K. Giant Radio Pulses from Pulsars. *Astrophys. Space Sci.* **2001**, *278*, 61–64. [[CrossRef](#)]

20. Mickaliger, M.B.; McEwen, A.E.; McLaughlin, M.A.; Lorimer, D.R. A study of single pulses in the Parkes Multibeam Pulsar Survey. *Mon. Not. R. Astron. Soc.* **2018**, *479*, 5413–5422. [[CrossRef](#)]
21. Raithel, C.A.; Shannon, R.M.; Johnston, S.; Kerr, M. Two Radio-emission Mechanisms in PSR J0901-4624. *Astrophys. J.* **2015**, *804*, L18. [[CrossRef](#)]
22. Staelin, D.H.; Reifenstein, E.C., III. Pulsating Radio Sources near the Crab Nebula. *Science* **1968**, *162*, 1481–1483. [[CrossRef](#)]
23. Kuiack, M.; Wijers, R.A.M.J.; Rowlinson, A.; Shulevski, A.; Huizinga, F.; Molenaar, G.; Prasad, P. Long-term study of extreme giant pulses from PSR B0950+08 with AARTFAAC. *Mon. Not. R. Astron. Soc.* **2020**, *497*, 846–854. [[CrossRef](#)]
24. Tsai, J.-W.; Simonetti, J.H.; Akukwe, B.; Bear, B.; Cutchin, S.E.; Dowell, J.; Gough, J.D.; Kanner, J.; Kassim, N.E.; Schinzel, F.K.; et al. Observations of Giant Pulses from Pulsar B0950+08 Using LWA1. *Astron. J.* **2015**, *149*, 65. [[CrossRef](#)]
25. Tsai, W., Jr.; Simonetti, J.H.; Akukwe, B.; Bear, B.; Gough, J.D.; Shawhan, P.; Kavic, M. Simultaneous Observations of Giant Pulses from Pulsar PSR B0950+08 at 42 MHz and 74 MHz. *Astron. J.* **2016**, *151*, 28. [[CrossRef](#)]
26. Cairns, I.H.; Johnston, S.; Das, P. Intrinsic variability and field statistics for pulsars B1641-45 and B0950+08. *Mon. Not. R. Astron. Soc.* **2004**, *353*, 270–286. [[CrossRef](#)]
27. Smirnova, T.V. Giant pulses from the pulsar PSR B0950+08. *Astron. Rep.* **2012**, *56*, 430–440. [[CrossRef](#)]
28. Singal, A.K.; Vats, H.O. Giant-pulse Emission from PSR B0950+08. *Astron. J.* **2012**, *144*, 155–162. [[CrossRef](#)]
29. Li, D.; Wang, P.; Qian, L.; Krco, M.; Jiang, P.; Yue, Y.; Jin, C.; Zhu, Y.; Pan, Z.; Nan, R.; et al. FAST in Space: Considerations for a Multibeam, Multipurpose Survey Using China’s 500-m Aperture Spherical Radio Telescope (FAST). *IEEE Microw. Mag.* **2018**, *19*, 112–119. [[CrossRef](#)]
30. Manchester, R.N.; Hobbs, G.B.; Teoh, A.; Hobbs, M. The Australia Telescope National Facility Pulsar Catalogue. *Astron. J.* **2005**, *129*, 1993–2006. [[CrossRef](#)]
31. Hotan, A.W.; van Straten, W.; Manchester, R.N. PSRCHIVE and PSRFITS: An Open Approach to Radio Pulsar Data Storage and Analysis. *Publ. Astron. Soc. Aust.* **2004**, *21*, 302–309. [[CrossRef](#)]
32. Rejep, R.; Yan, W.-M.; Wang, N. Simultaneous 50 cm/10 cm Single-pulse Polarization Observations of PSR J0953+0755. *Res. Astron. Astrophys.* **2022**, *22*, 065005. [[CrossRef](#)]
33. Gupta, Y.; Rickett, B.J.; Coles, W.A. Refractive Interstellar Scintillation of Pulsar Intensities at 74 MHz. *Astrophys. J.* **1993**, *403*, 183. [[CrossRef](#)]
34. Kazantsev, A.N.; Basalaeva, M.Y. Low-frequency observations of giant pulses from ordinary pulsars. *Mon. Not. R. Astron. Soc.* **2022**, *513*, 4332–4340. [[CrossRef](#)]
35. Pilkington, J.D.H.; Hewish, A.; Bell, S.J.; Cole, T.W. Observations of some further Pulsed Radio Sources. *Nature* **1968**, *218*, 126–129. [[CrossRef](#)]
36. Hankins, T.H.; Rickett, B.J. Frequency Dependence of Pulsar Profiles. *Astrophys. J.* **1986**, *311*, 684. [[CrossRef](#)]
37. Lyne, A.G.; Manchester, R.N. The shape of pulsar radio beams. *Mon. Not. R. Astron. Soc.* **1988**, *234*, 477–508. [[CrossRef](#)]
38. Manchester, R.N.; Lyne, A.G. Pulsar interpulses—Two poles or one? *Mon. Not. R. Astron. Soc.* **1977**, *181*, 761–767. [[CrossRef](#)]
39. Maciesiak, K.; Gil, J.; Ribeiro, V.A.R.M. On the pulse-width statistics in radio pulsars—I. Importance of the interpulse emission. *Mon. Not. R. Astron. Soc.* **2011**, *414*, 1314–1328. [[CrossRef](#)]
40. Kramer, M.; Johnston, S.; van Straten, W. High-resolution single-pulse studies of the Vela pulsar. *Mon. Not. R. Astron. Soc.* **2002**, *334*, 523–532. [[CrossRef](#)]
41. Sutton, J.M. Scattering of pulsar radiation in the interstellar medium. *Mon. Not. R. Astron. Soc.* **1971**, *155*, 51. [[CrossRef](#)]
42. Kazantsev, A.N.; Potapov, V.A. Search for giant pulses of radio pulsars at frequency 111 MHz with LPA radio telescope. *Res. Astron. Astrophys.* **2018**, *18*, 097. [[CrossRef](#)]
43. Lyubarsky, Y. Radio emission of the Crab and Crab-like pulsars. *Mon. Not. R. Astron. Soc.* **2019**, *483*, 1731–1736. [[CrossRef](#)]

**Disclaimer/Publisher’s Note:** The statements, opinions and data contained in all publications are solely those of the individual author(s) and contributor(s) and not of MDPI and/or the editor(s). MDPI and/or the editor(s) disclaim responsibility for any injury to people or property resulting from any ideas, methods, instructions or products referred to in the content.